

Strong vortex pinning in Co-doped BaFe₂As₂ single crystal thin films

C. Tarantini,^{1,a)} S. Lee,² Y. Zhang,³ J. Jiang,¹ C. W. Bark,² J. D. Weiss,¹ A. Polyanskii,¹ C. T. Nelson,³ H. W. Jang,² C. M. Folkman,² S. H. Baek,² X. Q. Pan,³ A. Gurevich,¹ E. E. Hellstrom,¹ C. B. Eom,² and D. C. Larbalestier¹

¹Applied Superconductivity Center, National High Magnetic Field Laboratory, Florida State University, Tallahassee, Florida 32310, USA

²Department of Materials Science and Engineering, University of Wisconsin–Madison, Madison, Wisconsin 53706, USA

³Department of Materials Science and Engineering, University of Michigan, Ann Arbor, Michigan 48109, USA

(Received 19 February 2010; accepted 17 March 2010; published online 8 April 2010)

We report the field and angular dependences of J_c of truly epitaxial Co-doped BaFe₂As₂ thin films grown on SrTiO₃/(La,Sr)(Al,Ta)O₃ with different SrTiO₃ template thicknesses. The films show J_c comparable to single crystals and a maximum pinning force $F_p(0.6T_c) > 5$ GN/m³ at $H/H_{irr} \sim 0.5$ indicative of strong high-field vortex pinning. Due to the strong correlated c -axis pinning, J_c for field along the c -axis exceeds J_c for $H\parallel ab$ plane, inverting the expectation of the H_{c2} anisotropy. High resolution transmission electron microscopy reveals that the strong vortex pinning is due to a high density of nanosize columnar defects. © 2010 American Institute of Physics.

[doi:10.1063/1.3383237]

The discovery of superconductivity in the ferropnictides has aroused great interest due to their high critical temperature T_c up to 56 K,^{1–4} very high upper critical fields H_{c2} together with the relatively low anisotropy ($\gamma \sim 1–6$) and irreversibility field H_{irr} close to H_{c2} .^{5,6} However, the presence of secondary phases at grain boundaries (GBs) in bulk materials^{7,8} initially hindered the investigation of the true intragrain critical current density J_c . Epitaxial films allow one to understand many fundamental properties including the limits of J_c , giving a much better view of the true potential of ferropnictides for applications. The deposition of 1111 (REFeAsO) thin films has been particular challenging due to the difficulties of controlling the fluorine content,⁹ whereas in the 122 (BaFe₂As₂) the growth conditions can be better controlled due to the low vapor pressure of cobalt.^{10–12} In several recent studies^{11,13,14} of both 1111 and 122 pnictides the maximum self-field J_c at 5 K was about 10 kA/cm², two to three orders of magnitude lower than in single crystal samples.⁶ Recently we have deposited high quality Ba-122 epitaxial thin films using a template engineering method, which enabled us to avoid weak-linked GBs.^{15,16}

In this paper, we study the effect of the SrTiO₃ (STO) template on the superconducting properties of Co-doped Ba-122 thin films, focusing on the interesting J_c properties caused by strong vortex pinning. We performed transport measurements of $J_c(H)$ and its angular dependence $J_c(\theta)$, correlating them to the structural properties determined by high resolution transmission electron microscopy (TEM). The 350 nm Co-doped Ba-122 films were grown on (001)-oriented (La,Sr)(Al,Ta)O₃ (LSAT) substrates using an intermediate template of 50–150 unit cells (u.c.) of SrTiO₃. All layers were grown by pulsed laser deposition, as reported in detail elsewhere.^{15,16} Figure 1 shows the superconducting transitions for which the critical temperature $T_{c,\rho=0}$ increases from 18.5 to 20.5 K upon increasing the STO template thick-

ness from 50 to 100 u.c. A further increase in the STO thickness results in a small reduction in T_c . The θ - 2θ patterns investigated by four-circle x-ray diffraction reveal only 00 l reflections indicative of a c -axis growth, while the φ -scans confirm that a single in-plane orientation dominates in all films.

The field dependencies of $J_c(T,H)$ for all the films are shown in Fig. 2. Both $J_c(H)$ and the irreversibility field H_{irr} are enhanced by increasing the STO thickness from 50 to 100 u.c. For instance, the self-field J_c at 12 K doubles its value reaching $J_c > 0.1$ MA/cm², while $H_{irr}(12$ K) determined by the Kramer extrapolation improves from about 18 T (in both field orientations) to 20–24 T ($H\parallel c$ and $H\parallel ab$, respectively). The film on 150 u.c. STO/LSAT shows a field dependence of J_c similar to the 100 u.c. film but J_c is slightly suppressed by its lower T_c . The lower-temperature J_c curves have comparatively weak field dependence up to 10–12 T due to their high H_{irr} but it is even more striking that J_c for $H\parallel c$ is always larger than J_c for $H\parallel ab$. Consistent with H_{c2} being higher for $H\parallel ab$, a crossover between $J_c(H\parallel c)$ and $J_c(H\parallel ab)$ is observed or estimated at the highest fields (e.g.,

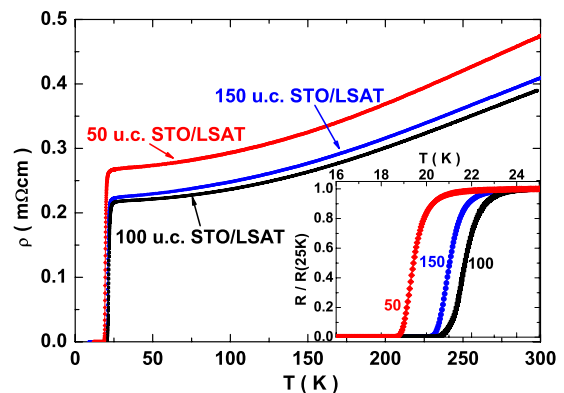


FIG. 1. (Color online) Resistivity vs temperature for the three characterized samples.

^{a)}Electronic mail: tarantini@asc.magnet.fsu.edu.

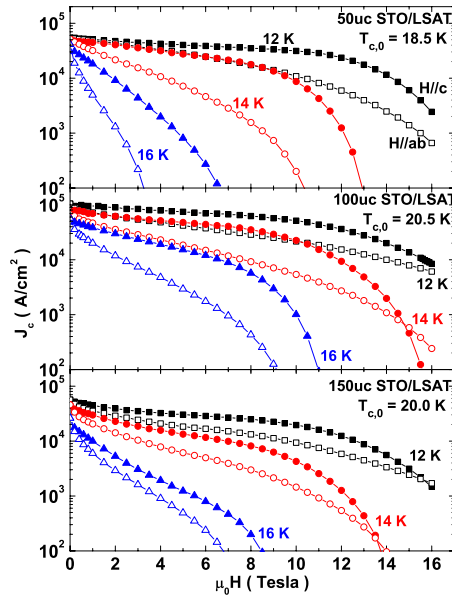


FIG. 2. (Color online) J_c as a function of $\mu_0 H$ for the samples on 50, 100, and 150 u.c. STO/LSAT. Open symbols denote H||*ab*, solid H||*c*.

~ 15 T and 14 K or at ~ 17 T and 12 K in 100 u.c. STO/LSAT film), which indicates strong pinning along the *c*-axis. However this crossover seems to be absent for the 50 u.c. STO/LSAT film for which the irreversibility field along the *c*-axis exceeds $H_{irr}^{||ab}$. The strong *c*-axis pinning effectiveness is emphasized by the temperature-normalized pinning force curves ($T \sim 0.6T_c$) in Fig. 3. The 100 u.c. STO/LSAT exhibits a remarkable $F_{p,max}$ above 5 GN/m^3 at about 9.5 T, which is better than for optimized Nb_3Sn at 4.2 K. For the 50 u.c. STO/LSAT film the maximum pinning force $F_{p,max} \sim 3.5 \text{ GN/m}^3$ occurs even at higher field ~ 12.5 T.

Figure 4 compares the normalized pinning forces $F_p/F_{p,max}$ as a function of the reduced magnetic field $h = H/H_{irr}$ at different temperatures for the best sample (100 u.c. STO/LSAT). For H||*ab* [Fig. 4(a)], the pinning force is maximum at $h_{max} \sim 0.2$ at 16 K but h_{max} increases at lower T. This trend suggests that higher temperature pinning is weakened by thermal fluctuations of vortices. At lower temperatures, the role of thermal fluctuations diminishes and h_{max} increases to ~ 0.3 – 0.4 . For H||*c* [Fig. 4(b)], $F_{p,max}$ at 16 K occurs already at $h_{max} \sim 0.4$ while at lower temperatures the curves superimpose with a peak at about $h_{max} \sim 0.5$. This behavior implies strong vortex core pinning by a dense array of nanoscale defects aligned along the *c* axis which reduce the effect of thermal fluctuations.

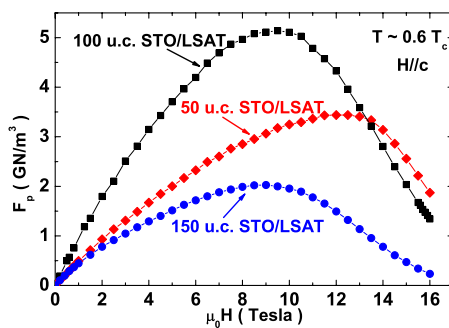


FIG. 3. (Color online) Pinning force as a function of field (H||*c*) at the same reduced temperature for the samples on 50, 100, and 150 u.c. STO/LSAT.

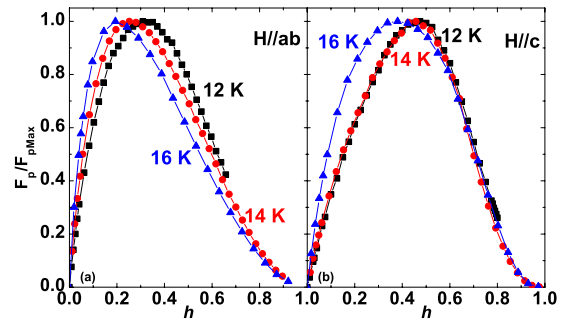


FIG. 4. (Color online) Normalized pinning force as a function of reduced field varying temperature for the film on 100 u.c. STO/LSAT.

To study the mechanisms of the crossover between $J_c(H||c)$ and $J_c(H||ab)$, we also measured the angular dependences of $J_c(\theta)$ shown in Fig. 5. For all magnetic fields, $J_c(\theta)$ of the sample on 100 u.c. STO/LSAT exhibits a strong and broad *c*-axis peak. Since $H_{c2}^{||ab}$ is larger than $H_{c2}^{||c}$, such behavior is opposite to what is expected from the mass anisotropy. At low fields pinning becomes effective over all θ , significantly flattening $J_c(\theta)$. At larger fields, the *c*-axis peak still remains pronounced but in a smaller range around 0° so the *ab*-plane peak due to the mass anisotropy emerges.

The microstructural origin of strong vortex pinning was revealed by TEM images, shown in Fig. 6. The planar view of the 122 film grown on 100 u.c. STO/LSAT shows a high density of randomly distributed defects with average diameter of 5 nm. The inset of Fig. 6 shows they are columnar defects vertically aligned which grow from the template with only a slight meandering. From the planar view TEM, we estimated a mean separation of 16–17 nm corresponding to a matching field of about 7–8 T, comparable to the peak position of the pinning force. The estimated volume fraction $\sim 8\%$ is smaller than the critical concentration $\sim 10\%$ above which current blocking by pins starts decreasing $F_{p,max}$ (Ref. 17) so J_c of our films could be further increased by more columnar pins. For H||*c*, $F_p(h)$ at low temperatures follows the scaling behavior $F_p(h) \propto h^p(1-h)^q$ with $p \approx q \approx 1$ and the maximum F_p at $h = H/H_{irr} \approx 0.5$, indicating strong core pinning of vortices. For H||*ab*, the exponents $p \approx 0.65$ and $q \approx 2.32$ at 16 K and $p \approx 0.8$ and $q \approx 2.24$ at 14 K seem to suggest collective pinning affected by thermal fluctuations of vortices. The columnar defects may be correlated with oxygen incorporation during film growth. Wavelength dispersive x-ray spectroscopy indicates typical whole-film composition ratios of Ba:Fe:Co:As:O = 1:1.7:0.13:1.7:0.3. On the other hand, both x-ray energy dispersive spectroscopy and

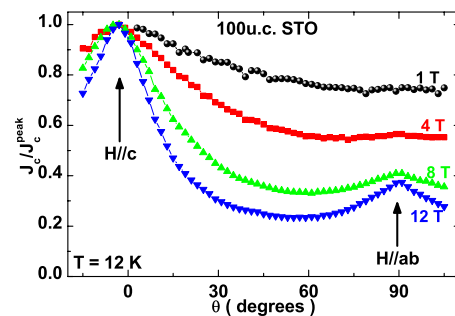


FIG. 5. (Color online) Normalized $J_c(\theta, 12 \text{ K})$ at different applied field for the film on 100 u.c. STO/LSAT.

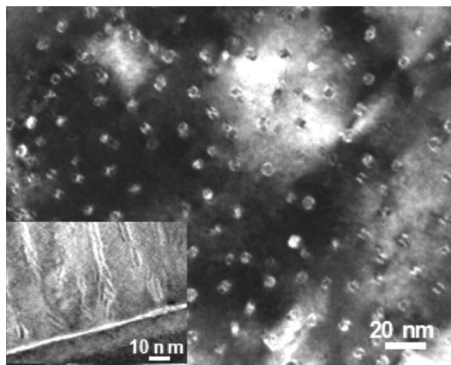


FIG. 6. Planar view TEM of 100 u.c. STO/LSAT. In the inset a cross section of the 50 u.c. STO/LSAT.

electron energy-loss spectroscopy in planar TEM images reveal that the line defects mainly consist of a Ba–Fe–O secondary phase, depleted of As, suggesting that they are O-rich defects that compensate the As deficiency. Further experiments to test this hypothesis are under way.

The effectiveness of the templated substrate is evident by comparing $J_c(H, T, \theta)$ of our samples with other thin film reports. For instance, Sr-122 thin films grown on different substrates and exhibiting good XRD patterns had $T_{c,p=0} \sim 15\text{--}16$ K, $\Delta T_c \sim 2\text{--}3$ K, and $J_c \approx 10\text{--}20$ kA/cm² at 4–5 K.^{10,11,13} By contrast we obtained $J_c \sim 0.1$ MA/cm² at 12 K in our best sample. Another striking feature of our films is their very strong vortex pinning for H||c. Recently Iida *et al.*¹⁸ reported angular dependences and TEM of high quality Ba-122 thin film on LSAT substrates. They observed no GB or other defects but, as expected in very clean samples, J_c shows no *c*-axis peak and is low due to the lack of correlated pinning. Unlike the angular dependence data reported by Maiorov *et al.*¹³ where a *c*-axis peak was observed only up to 1 T, our data show that for H||c, pinning remains effective up to the maximum field measured (16 T). Such strong vortex pinning by a high density of columnar defects whose matching field is close to the maximum of $F_p(H)$ also reduces thermal fluctuations. Taken together, these studies suggest that vortex pinning in 122 is really versatile, and also that it is important to suppress granular effects to understand the high J_c of which the system is capable.

The comparison between films grown on STO templates of different thickness reveals that a further improvement of the superconducting properties is still possible. In fact, whereas the 100 u.c. STO/LSAT sample has the highest T_c and largest J_c , the best pinning conditions are reached in the 50 u.c. STO/LSAT where the maximum of the pinning force occurs close to H_{irr} ($h_{max} \sim 0.6$) and $H_{irr}^{||c} > H_{irr}^{||ab}$ over the whole measured temperature and field ranges. Increasing the

pin volume fraction by optimizing the 122 growth conditions without T_c suppression seems quite feasible.

Work at NHMFL was supported under NSF Cooperative Agreement No. DMR-0084173, by the State of Florida, and by AFOSR Grant No. FA9550-06-1-0474. Work at the University of Wisconsin was supported by funding from the DOE Office of Basic Energy Sciences under Award No. DE-FG02-06ER46327. TEM work at the University of Michigan was supported by the DOE Grant No. DE-FG02-07ER46416. TEM facility was supported by NSF.

¹Y. Kamihara, T. Watanabe, M. Hirano, and H. Hosono, *J. Am. Chem. Soc.* **130**, 3296 (2008).

²X. H. Chen, T. Wu, G. Wu, R. H. Liu, H. Chen, and D. F. Fang, *Nature (London)* **453**, 761 (2008).

³C. Wang, L. Li, S. Chi, Z. Zhu, Z. Ren, Y. Li, Y. Wang, X. Lin, Y. Luo, S. Jiang, X. Xu, G. Cao, and Z. Xu, *EPL* **83**, 67006 (2008).

⁴M. Rotter, M. Tegel, and D. Johrendt, *Phys. Rev. Lett.* **101**, 107006 (2008).

⁵F. Hunte, J. Jaroszynski, A. Gurevich, D. C. Larbalestier, R. Jin, A. S. Sefat, M. A. McGuire, B. C. Sales, D. K. Christen, and D. Mandrus, *Nature (London)* **453**, 903 (2008).

⁶A. Yamamoto, J. Jaroszynski, C. Tarantini, L. Balicas, J. Jiang, A. Gurevich, D. C. Larbalestier, R. Jin, A. S. Sefat, M. A. McGuire, B. C. Sales, D. K. Christen, and D. Mandrus, *Appl. Phys. Lett.* **94**, 062511 (2009).

⁷A. Yamamoto, J. Jiang, C. Tarantini, N. Craig, A. A. Polyanskii, F. Kametani, F. Hunte, J. Jaroszynski, E. E. Hellstrom, D. C. Larbalestier, R. Jin, A. S. Sefat, M. A. McGuire, B. C. Sales, D. K. Christen, and D. Mandrus, *Appl. Phys. Lett.* **92**, 252501 (2008).

⁸A. Yamamoto, A. A. Polyanskii, J. Jiang, F. Kametani, C. Tarantini, F. Hunte, J. Jaroszynski, E. E. Hellstrom, P. J. Lee, A. Gurevich, D. C. Larbalestier, Z. A. Ren, J. Yang, X. L. Dong, W. Lu, and Z. X. Zhao, *Supercond. Sci. Technol.* **21**, 095008 (2008).

⁹H. Hiramatsu, T. Katase, T. Kamiya, M. Hirano, and H. Hosono, *Appl. Phys. Lett.* **93**, 162504 (2008).

¹⁰H. Hiramatsu, T. Katase, T. Kamiya, M. Hirano, and H. Hosono, *Appl. Phys. Express* **1**, 101702 (2008).

¹¹E. M. Choi, S. G. Jung, N. H. Lee, Y. S. Kwon, W. N. Kang, D. H. Kim, M. H. Jung, S. I. Lee, and L. Sun, *Appl. Phys. Lett.* **95**, 062507 (2009).

¹²K. Iida, J. Hänisch, R. Hühne, F. Kurth, M. Kidszun, S. Haindl, J. Werner, L. Schultz, and B. Holzapfel, *Appl. Phys. Lett.* **95**, 192501 (2009).

¹³B. Maiorov, S. A. Baily, Y. Kohama, H. Hiramatsu, L. Civale, M. Hirano, and H. Hosono, *Supercond. Sci. Technol.* **22**, 125011 (2009).

¹⁴S. Haindl, M. Kidszun, A. Kauffmann, K. Nenkov, N. Kozlova, J. Freudenberger, T. Thersleff, J. Werner, E. Reich, L. Schultz, and B. Holzapfel, *Phys. Rev. Lett.* **104**, 077001 (2010).

¹⁵S. Lee, J. Jiang, J. D. Weiss, C. M. Folkman, C. W. Bark, C. Tarantini, A. Xu, D. Abrahimov, A. Polyanskii, C. T. Nelson, Y. Zhang, S. H. Baek, H. W. Jang, A. Yamamoto, F. Kametani, X. Q. Pan, E. E. Hellstrom, A. Gurevich, C. B. Eom, and D. C. Larbalestier, *Appl. Phys. Lett.* **95**, 212505 (2009).

¹⁶S. Lee, J. Jiang, Y. Zhang, C. W. Bark, J. D. Weiss, C. Tarantini, C. T. Nelson, H. W. Jang, C. M. Folkman, S. H. Baek, A. Polyanskii, D. Abrahimov, A. Yamamoto, J. W. Park, X. Q. Pan, E. E. Hellstrom, D. C. Larbalestier, and C. B. Eom, *Nature Mater.* (unpublished).

¹⁷A. Gurevich, *Supercond. Sci. Technol.* **20**, S128 (2007).

¹⁸K. Iida, J. Hänisch, T. Thersleff, F. Kurth, M. Kidszun, S. Haindl, R. Hühne, L. Schultz, and B. Holzapfel, *Phys. Rev. B* **81**, 100507(R) (2010).